ISA Transactions 91 (2019) 78–89

Contents lists available at ScienceDirect

ISA Transactions

journal homepage: www.elsevier.com/locate/isatrans

Research article

Active nonlinear partial-state feedback control of contacting force for a pantograph–catenary system

Bing Zhu [a,*], Zhiling Ren [b], Wenjing Xie [c], Fengyi Guo [b], Xiaohua Xia [d]

[a] The Seventh Research Division, Beihang University, Beijing 100191, PR China
[b] Faculty of Electrical and Control Engineering, Liaoning Technical University, Huludao 125105, PR China
[c] School of Computer and Information Science, Southwest University, Chongqing 400715, PR China
[d] Department of Electrical, Electronic and Computer Engineering, University of Pretoria, Pretoria 0028, South Africa

HIGHLIGHTS

- The backstepping approach is firstly applied to control design for pantograph–catenary system.
- The closed-loop system is capable of tracking not only constant reference contacting force but also time-varying periodic reference forces.
- A high-order differentiator is designed to approximate the unknown derivatives of time-varying elasticity coefficient.
- A simple observer is designed to reconstruct the un-measurable system states.

ARTICLE INFO

Article history:
Received 11 May 2018
Received in revised form 16 October 2018
Accepted 25 January 2019
Available online 12 February 2019

Keywords:
Pantograph–catenary system
Backstepping
Trajectory tracking
Observer

ABSTRACT

In this paper, a nonlinear partial-state feedback control is designed for a 3-DOF pantograph–catenary system by using backstepping approach, such that the contacting force of the closed-loop system is capable of tracking its reference profile. In the control design, the pantograph–catenary model is transformed into a triangular form, facilitating the utilization of backstepping. Derivatives of virtual controls in backstepping are calculated explicitly. A high-order differentiator is designed to estimate the unknown time derivatives of elasticity coefficient; and an observer is proposed to reconstruct the unmeasurable states. It can be proved theoretically that, with the proposed nonlinear partial-state feedback control, the tracking error of the contacting force is ultimately bounded with tunable ultimate bounds. Theoretical results are demonstrated by numerical simulations.

1. Introduction

Pantograph–catenary system is prevailingly adopted in modern railway industry to supply electricity to high-speed trains. To guarantee that the high-speed train obtains stable electricity supply from the wires, a solid contact between pantograph and catenary is of great importance [1]. As pointed out in previous researches, the loss of contact would lead to insufficient supply of energy to the high-speed train, resulting in disfunctions in acceleration, braking and communication. In another aspect, however, with over-contacting force, there would be considerably arcing phenomenon or rapid wear in both pantograph and catenary, reducing significantly the duration of the entire system. Consequently, it is significantly necessary to maintain an appropriate contacting force between pantograph and catenary.

To maintain an optimal contacting force for the pantograph–catenary system is a challenging task, since there exist couplings and periodic nonlinearities in its dynamics [2] due to the high speed of the train. Influences resulted from couplings and periodic nonlinearities become especially negative, if the train speed is large such that the frequency of catenary stiffness variation is excessively high. The optimal contacting force between the pantograph and catenary can be calculated experimentally [3]. Active PID control strategy can be applied to maintaining a constant reference contacting force [4]. Other advanced control technologies that can be employed to the pantograph–catenary system include robust optimal control [5], feedback linearization [6], output-feedback regulation [7], output-feedback control with adaptive estimation [8], model predictive control [9], and an implementation-oriented technique named wire-actuated control with contact force estimation [10].

Some typical difficulties in active control design for pantograph–catenary system include that: (1) the elasticity coefficient of the catenary is time-varying, and the parameters in its mathematical model are unknown; and (2) some system states, such

* Corresponding author.
E-mail addresses: zhubing@buaa.edu.cn (B. Zhu), lngdrzl@163.com (Z. Ren), xiewenjing@swu.edu.cn (W. Xie), fyguo64@126.com (F. Guo), xxia@up.ac.za (X. Xia).

https://doi.org/10.1016/j.isatra.2019.01.033

as displacement velocities of the pantograph, are unmeasurable. For the time-varying elasticity coefficient of the catenary, it can be assumed that it is periodic, and some approximations have been proposed [10,11]; however, the approximated models cannot be directly used, because accuracy of the approximated model is un-assured, and some parameters are difficult to determine. To estimate the unmeasurable states, sliding mode observers have been proposed [7]; however, typical problems in sliding mode control (such as chattering) would arise.

Generally, there exist two types of pantograph–catenary system modeling, namely 2-DOF modeling [7,11–14] and 3-DOF modeling [5,10,15,16]. The 3-DOF model contains more dynamics (thus more accurate) than the 2-DOF model; however, it is comparatively complicated, and there exist more uncertain parameters or un-measurable states. In this paper, based on backstepping approach, a nonlinear partial-state feedback control is proposed for a 3-DOF pantograph–catenary system. The linear time-varying model of the pantograph–catenary system can be transformed into a cascaded form, and backstepping can be applied to serve as the fundamental structure of the proposed controller, such that the controller can be designed in steps for reduced-order subsystems. Another advantage of applying backstepping is to facilitate the design of observers for unmeasurable states, and to guarantee the stability of the closed-loop system. *Main contributions* of this paper include: (1) the backstepping approach is firstly applied to control 3-DOF pantograph–catenary system; (2) by using backstepping approach, the closed-loop system is capable of tracking not only constant reference contacting force but also time-varying periodic reference forces; (3) a high-order differentiator is designed to approximate the unknown derivatives of time-varying elasticity coefficient, such that usage of unknown time-varying elasticity coefficient model can be avoided; and (4) a simple observer is designed to reconstruct the unmeasurable system states. Ultimate boundedness of tracking errors of the closed-loop system can be proved. The theoretical results are validated by numerical simulations.

The layout of this paper is arranged as following. In Section 2, the mathematical model of the pantograph–catenary system is presented, and the objectives of control design are stated. In Section 3, a full-state feedback nonlinear backstepping control is described in detail, and asymptotic stability of the tracking error is proved theoretically. In Section 4, a high-order differentiator is designed to estimate the time derivatives of elasticity coefficient, and an observer is designed to reconstruct the unmeasurable system states; it is proved that the tracking error of the closed-loop system with the proposed partial-state feedback control is ultimately bounded with tunable ultimate bounds. In Section 5, main theoretical results are demonstrated by numerical simulations, and corresponding discussions are given. The final section is the conclusion.

2. Problem statement

In this section, the pantograph–catenary system is modeled into a 3-DOF time-varying linear system. In the pantograph–catenary system, as depicted by Fig. 1, the pantograph is fixed on the top of the train, and runs in high-speed with the train. A supporting force is exerted on the lower frame of the pantograph from some actuators, and to generated a contacting force between the pan-head of the pantograph and the catenary, such that electrical power can be transferred from the catenary to the train through the pantograph.

Due to the high speed of the train, there exist some considerable vibrations in the catenary, and the contact force would be negatively influenced. Excessively large contact force would lead to extreme wear of the pan-head and the catenary, while too small

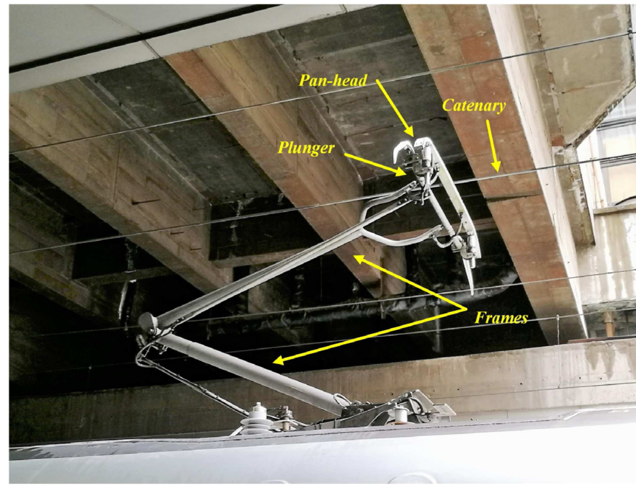

Fig. 1. Pantograph–catenary system equipped on a practical high-speed train.

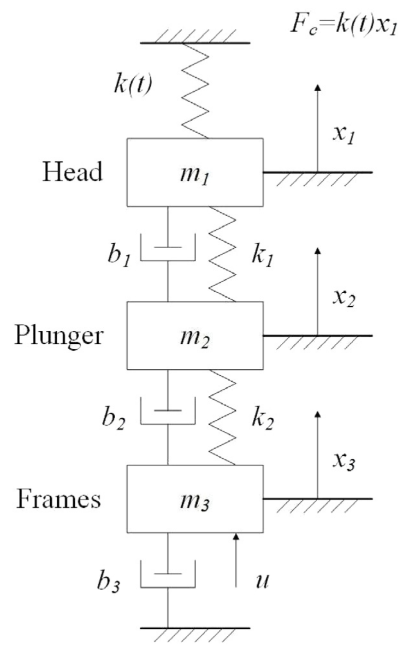

Fig. 2. Approximate structure of the pantograph–catenary system.

contact force would result in arcing phenomenon or even lost of contact. All of these situations will deteriorate the electricity supply for the train. Consequently, *the objective* of this paper is to design an active control for the pantograph, such that a proper reference contacting force can be maintained.

2.1. Mathematical model of pantograph–catenary system

The 3-DOF pantograph–catenary system is composed by a head, a plunger and frames. In this paper, the pantograph–catenary model under consideration is an under-actuated one, and it is different from the fully-actuated model in [5]. Its structure can be approximated by a mass-elasticity model, as is given in Fig. 2, where the active control u is only exerted on the lower frame. The dynamic equations of the 3-DOF pantograph–catenary system can be obtained by

$$\begin{cases} m_1\ddot{x}_1 = k_1(x_2-x_1)+b_1(\dot{x}_2-\dot{x}_1)-k(t)x_1, \\ m_2\ddot{x}_2 = -k_1(x_2-x_1)-k_2(x_2-x_3)-b_1(\dot{x}_2-\dot{x}_1)-b_2(\dot{x}_2-\dot{x}_3), \\ m_3\ddot{x}_3 = -k_2(x_3-x_2)-b_2(\dot{x}_3-\dot{x}_2)-b_3\dot{x}_3+u, \end{cases} \tag{1}$$

where m_1 and m_2 denote the mass of the pantograph head and the plunger, respectively; m_3 denotes the gross mass of the frames; x_1, x_2 and x_3 are the positions of the pantograph head, the plunger and the frames, respectively; k_1 and k_2 denote the elasticity constants of the plunger and the frames; b_1, b_2 and b_3 are the damping constants of the pantograph head, the plunger and the frames, respectively; t denotes the continuous time; $k(t)$ is the time-varying elasticity (or stiffness) coefficient between the pantograph head and the wire; and u is the control input.

The output of the pantograph–catenary system is the contacting force between the pantograph head and the wire:

$$F_c \triangleq k(t)x_1, \tag{2}$$

where the contacting force F_c is assumed to be measured directly, and the position x_1 can be measured, indicating that the value of the elasticity coefficient can be obtained by

$$k(t) = \frac{F_c}{x_1}. \tag{3}$$

However, it is supposed in this paper that the accurate physical model of the time-varying elasticity coefficient $k(t)$ is unknown.

The time-varying elasticity coefficient can be approximated by a high-order periodic model [11]:

$$k(t) = K_0 + \sum_{i=1}^{3} K_i \cos(\frac{2i\pi}{L}Vt) + K_7 \cos(\frac{14\pi}{L}Vt), \tag{4}$$

where K_i $(i = 0, 1, 2, 3, 7)$ are constant uncertain stiffness coefficients; V is the train speed; and L is the span length.

Remark 1. The contact force can be measured directly with strain gages, accelerometers and strain gage position sensors, as proposed in [17]. It has to be acknowledged that, the measurement might be somehow inaccurate in harsh environment. The contact force can also be estimated by using numerical methods, e.g., [11], but with fully-known elasticity coefficient.

Remark 2. Nonlinearities in the pantograph are neglected in this paper, and the pantograph is assumed to be a 3-DOF mass–spring–damper system with constant elasticity and damping coefficients. Please see [18] for more details.

Remark 3. The elasticity coefficient (4) of the catenary is time-varying due to vibrations of the contacting wire, and it can be expanded as Taylor Series. In quite a lot of previous researches, higher-order terms in Taylor Series are neglected, and only the first order periodic term is considered [5,6,8,13,14]. However, some researches claim that it is inaccuracy to consider only the first periodic term in the Taylor Series [11,16]. Consequently, more higher-order terms in Taylor Series are considered in this paper to improve the accuracy of the structure. In the Taylor Series of the catenary, parameters are unmeasurable and to be estimated.

2.2. Linear time-varying representation

The system model (1) can be transformed into a linear time-varying representation:

$$\begin{cases} \dot{z}_1 = z_2, \\ \dot{z}_2 = -\frac{k_1+k(t)}{m_1}z_1 - \frac{b_1}{m_1}z_2 + \frac{k_1}{m_1}z_3 + \frac{b_1}{m_1}z_4, \\ \dot{z}_3 = z_4, \\ \dot{z}_4 = \frac{k_1}{m_2}z_1 + \frac{b_1}{m_2}z_2 - \frac{k_1+k_2}{m_2}z_3 - \frac{b_1+b_2}{m_2}z_4 + \frac{k_2}{m_2}z_5 + \frac{b_2}{m_2}z_6, \\ \dot{z}_5 = z_6, \\ \dot{z}_6 = \frac{k_2}{m_3}z_3 + \frac{b_2}{m_3}z_4 - \frac{k_2}{m_3}z_5 - \frac{b_2+b_3}{m_3}z_6 + \frac{1}{m_3}u, \end{cases} \tag{5}$$

or

$$\dot{z} = A(t)z + bu,$$

where $z = [z_1, z_2, z_3, z_4, z_5, z_6]^T \triangleq [x_1, \dot{x}_1, x_2, \dot{x}_2, x_3, \dot{x}_3]^T$, and

$$A(t) = \begin{bmatrix} 0 & 1 & 0 & 0 & 0 & 0 \\ -\frac{k_1+k(t)}{m_1} & -\frac{b_1}{m_1} & \frac{k_1}{m_1} & \frac{b_1}{m_1} & 0 & 0 \\ 0 & 0 & 0 & 1 & 0 & 0 \\ \frac{k_1}{m_2} & \frac{b_1}{m_2} & -\frac{k_1+k_2}{m_2} & -\frac{b_1+b_2}{m_2} & \frac{k_2}{m_2} & \frac{b_2}{m_2} \\ 0 & 0 & 0 & 0 & 0 & 1 \\ 0 & 0 & \frac{k_2}{m_3} & \frac{b_2}{m_3} & -\frac{k_2}{m_3} & -\frac{b_2+b_3}{m_3} \end{bmatrix},$$

$$b = \begin{bmatrix} 0 \\ 0 \\ 0 \\ 0 \\ 0 \\ \frac{1}{m_3} \end{bmatrix}.$$

The output of the system can be given by

$$y = C(t)z, \tag{6}$$

where $y = F_c$, and $C(t) = [k(t), 0, 0, 0, 0, 0]$. System (5) is time-varying in existence of the time-varying elasticity coefficient $k(t)$.

2.3. Optimal contacting force with respect to mechanical wear and electrical resistance

The optimal contact force should achieve a tradeoff between material wear and electrical resistance of the pantograph–catenary system. The material wear decreases as the contact force decreases; meanwhile, decrease of the contact force would lead to larger electrical resistance between the pantograph and catenary, impeding the reliable currency transmission.

The material wear includes oxidational wear and melt wear. The oxidational wear model [19] of the contact wire can be given by

$$w_o(F_c) = f_m \left[\frac{\alpha_w \mu P_{eq}(F_c)}{L_{ox}} - \frac{A_n^{0.5} K_{ox} \left(T_m^{ox} - T_b\right) P_{eq}(F_c)^{0.5} n_{asp}^{0.5}}{L_{ox} H_0^{0.5} l_b v} \right], \tag{7}$$

where $w_o(F_c)$ denotes the wear of the contact wire, which is a function of the contacting force; f_m represents the volume fraction of molten material; α_w denotes the heat distribution coefficient; μ is the sliding friction coefficient of the contact wire material; L_{ox} denotes the latent heat of fusion per unit volume of oxide; A_n is the actual contact area; K_{ox} represents the thermal conductivity of oxide; T_m^{ox} denotes the melting temperature of the material; T_b is the bulk temperature; n_{asp} is the number of asperity in contact; H_0 denotes the hardness of material; l_b denotes the equivalent linear diffusion distance for bulk heating; and v is the actual velocity of the train. Some values of the above parameters can be found in [19,20]. The equivalent contact force $P_{eq}(F_c)$ is a function of the contact force F_c:

$$P_{eq}(F_c) = F_c + P_e = F_c + \frac{R_e}{\mu v} I^2, \tag{8}$$

where P_e is the equivalent electrical contact force; R_e denotes the electrical resistance at the contact point; and I is the electrical current transferred through the contact.

The melt wear model [19] of the contact wire is a function of the contacting force F_c, and it can be given by

$$w_m(F_c) = f_m \left[\frac{\alpha_w \mu P_{eq}(F_c)}{L_m} - \frac{A_n K_m \left(T_m - T_0\right)}{L_m l_b v} \right], \tag{9}$$

where L_m is the latent heat of fusion per unit volume for metal; K_m is the thermal conductivity of the metal material; T_m is the melting temperature of the metal material; and T_0 is the ambient temperature.

The electrical resistance with respect to contact force [21] can be calculated by

$$R_e(F_c) = \frac{\rho_1+\rho_2}{4}\sqrt{\frac{\pi H}{F_c}}, \tag{10}$$

where ρ_1 and ρ_2 are resistance rates of the pantograph and the catenary; and H is the contact hardness of the materials.

Based on (7)–(10), the cost function to calculate the optimal contact force can be constructed by

$$J(F_c) = q_1 w_o(F_c) + q_2 w_m(F_c) + q_3 R_e(F_c), \tag{11}$$

where q_1, q_2 and q_3 are positive weight parameters for optimization. The optimal contact force can be calculated by

$$F_c^* = \arg\min_{F_c} J(F_c), \tag{12}$$

subject to (7)–(10).

The value of optimal contacting force may vary from case to case with respect to different values of parameters in various pantograph–catenary projects. Detailed value of pantograph–catenary parameters can be found in examples in [11,22,23] Generally, the optimal contacting force is often constant, and its value is around 100–120 N [23].

Remark 4. It has to be admitted that, in this paper, no systematic way of selecting weight parameters can be given. Parameter selecting has to be processed through trials. Different values of weight parameters reflect different emphasis on electricity resistance (contact force) or wear. For example, with the values of parameters provided in [19] and the weight parameters $q_1 = 0.2$, $q_2 = 1$ and $q_3 = 0.5$, it can be calculated that the optimal contacting force should be $F_c^* = 109.7$N.

Remark 5. The optimization (12) can be solved by using MATLAB function "`fmincon`".

2.4. Control objective

Suppose that, in this research, the contact force (F_c) and the positions (x_1, x_2 and x_3, or z_1, z_3 and z_5) can be measured directly. However, in practical cases, the velocities ($\dot{x}_1, \dot{x}_2$ and $\dot{x}_3$, or z_2, z_4 and z_6) are often unmeasurable. Moreover, the stiffness coefficients (K_i) are uncertain constant parameters.

Remark 6. Although corresponding devices are fairly expensive, the contact force is measurable indeed. There exist some researches on estimation of contact force without using the expensive devices [10,11].

The *objective* of this paper is to design a nonlinear control for the pantograph–catenary system with unmeasurable displacement variations and uncertain stiffness coefficients, such that the output of the system is capable of tracking a constant reference contacting force with small tracking error:

$$\lim_{t\to+\infty} |y(t) - y_r| < \epsilon, \tag{13}$$

where $y_r = F_c^*$ is the reference contacting force, and $\epsilon > 0$ is a small positive number.

3. Full-state feedback nonlinear control

In this section, a full-state feedback nonlinear control is designed to give a fundamental structure of the proposed partial-state feedback control. In the next section, differentiators and state observers will be designed to replace the uncertain parameters and unmeasurable states.

To facilitate control design, the time-varying model is transformed into a triangular form (the definition of triangular system can be referred to [24]). The nonlinear control is designed through backstepping [25], with derivatives of virtual controls calculated explicitly. Asymptotic stability of tracking errors of the closed-loop system is proved theoretically.

3.1. Model transformation

Define manifolds:

$$\xi_1 = k_1 z_3 + b_1 z_4, \tag{14}$$

$$\xi_2 = k_2 z_5 + b_2 z_6. \tag{15}$$

It follows from (5), (14) and (15) that the 3-DOF model can be transformed into a triangular form

$$\begin{cases} \dot{z}_1 &= z_2, \\ \dot{z}_2 &= -\frac{k_1+k(t)}{m_1} z_1 - \frac{b_1}{m_1} z_2 + \frac{1}{m_1}\xi_1, \\ \dot{\xi}_1 &= k_1 z_4 + b_1\left(\frac{k_1}{m_2} z_1 + \frac{b_1}{m_2} z_2 - \frac{k_1+k_2}{m_2} z_3 - \frac{b_1+b_2}{m_2} z_4 + \frac{1}{m_2}\xi_2\right), \\ \dot{\xi}_2 &= k_2 z_6 + b_2\left(\frac{k_2}{m_3} z_3 + \frac{b_2}{m_3} z_4 - \frac{k_2}{m_3} z_5 - \frac{b_2+b_3}{m_3} z_6 + \frac{1}{m_3} u\right), \end{cases} \tag{16}$$

with internal dynamics given by

$$\begin{cases} \dot{z}_3 &= -\frac{k_1}{b_1} z_3 + \frac{1}{b_1}\xi_1, \\ \dot{z}_5 &= -\frac{k_2}{b_2} z_5 + \frac{1}{b_2}\xi_2. \end{cases} \tag{17}$$

Remark 7. It can be seen from (17) that the internal dynamics is actually a linear stable system

$$\begin{cases} \dot{z}_3 &= -\frac{k_1}{b_1} z_3, \\ \dot{z}_5 &= -\frac{k_2}{b_2} z_5. \end{cases} \tag{18}$$

plus inputs $\frac{1}{b_1}\xi_1$ and $\frac{1}{b_2}\xi_2$.

In another aspect, based on (6), it holds that

$$x_1 = z_1 = \frac{y}{k(t)}.$$

Then, an auxiliary reference profile can be defined:

$$z_{1r} \triangleq \frac{y_r}{k(t)}.$$

The objective is then to design control for the triangular system (16)–(17), such that

$$\lim_{t\to+\infty} |z_1(t) - z_{1r}(t)| < \frac{\epsilon}{\sup_{t\to+\infty}(|k(t)|)}. \tag{19}$$

3.2. Control design by using backstepping

The nonlinear control for (16)–(17) is designed step by step via backstepping in this section.

Step 1: Define tracking error $e_1 = z_1 - z_{1r}$. It follows that

$$\dot{e}_1 = \dot{z}_1 - \dot{z}_{1r} = z_2 - \dot{z}_{1r} = e_2 + \alpha_1 - \dot{z}_{1r},$$

where $e_2 \triangleq z_2 - \alpha_1$, and α_1 is the virtual control to be tracked by z_2. Design the virtual control

$$\alpha_1 = -c_1 e_1 + \dot{z}_{1r}, \tag{20}$$

where $c_1 > 0$ is a constant control gain. It then follows that

$$\dot{e}_1 = -c_1 e_1 + e_2. \tag{21}$$

Select the Lyapunov candidate $L_1 = \frac{1}{2}e_1^2$. Its time derivative can be calculated by

$$\dot{L}_1 = -c_1 e_1^2 + e_1 e_2, \tag{22}$$

where $-c_1 e_1^2$ is negative definite, and $e_1 e_2$ is to be canceled in the next step.

Step 2: The time derivative of e_2 can be calculated by

$$\begin{aligned}\dot{e}_2 =& \dot{z}_2 - \dot{\alpha}_1\\ =& -\frac{k_1+k(t)}{m_1}z_1 - \frac{b_1}{m_1}z_2 + \frac{1}{m_1}\xi_1 - \dot{\alpha}_1\\ =& -\frac{k_1+k(t)}{m_1}z_1 - \frac{b_1}{m_1}z_2 - \dot{\alpha}_1 + e_3 + \alpha_2,\end{aligned}$$

where $e_3 \triangleq \frac{1}{m_1}\xi_1 - \alpha_2$, and α_2 is the virtual control to be tracked by $\frac{1}{m_1}\xi_1$. Design the virtual control

$$\alpha_2 = -e_1 - c_2 e_2 + \frac{k_1+k(t)}{m_1}z_1 + \frac{b_1}{m_1}z_2 + \dot{\alpha}_1, \tag{23}$$

where $c_2 > 0$ is a constant control gain. It then follows that

$$\dot{e}_2 = -e_1 - c_2 e_2 + e_3.$$

Select the Lyapunov candidate $L_2 = L_1 + \frac{1}{2}e_2^2$. Its time derivative can be calculated by

$$\dot{L}_1 = -c_1 e_1^2 - c_2 e_2^2 + e_2 e_3,$$

where $-c_1 e_1^2 - c_2 e_2^2$ is negative definite, $e_1 e_2$ in (22) is canceled, and $e_2 e_3$ is to be canceled in the next step.

Step 3: The time derivative of e_3 can be calculated by

$$\begin{aligned}\dot{e}_3 =& \frac{1}{m_1}\dot{\xi}_1 - \dot{\alpha}_2\\ =& \frac{b_1}{m_1}\left(\frac{k_1}{m_2}z_1 + \frac{b_1}{m_2}z_2 - \frac{k_1+k_2}{m_2}z_3 - \frac{b_1+b_2}{m_2}z_4\right)\\ &+ \frac{k_1}{m_1}z_4 - \dot{\alpha}_2 + \frac{b_1}{m_1}\frac{1}{m_2}\xi_2\\ =& \frac{b_1}{m_1}\left(\frac{k_1}{m_2}z_1 + \frac{b_1}{m_2}z_2 - \frac{k_1+k_2}{m_2}z_3 - \frac{b_1+b_2}{m_2}z_4\right)\\ &+ \frac{k_1}{m_1}z_4 - \dot{\alpha}_2 + e_4 + \alpha_3.\end{aligned}$$

where α_3 is the virtual control to be tracked by $\frac{b_1}{m_1 m_2}\xi_2$, and $e_4 \triangleq \frac{b_1}{m_1 m_2}\xi_2 - \alpha_3$.

Design the virtual control

$$\begin{aligned}\alpha_3 =& -e_2 - c_3 e_3 + \dot{\alpha}_2 - \frac{k_1}{m_1}z_4\\ &- \frac{b_1}{m_1}\left(\frac{k_1}{m_2}z_1 + \frac{b_1}{m_2}z_2 - \frac{k_1+k_2}{m_2}z_3 - \frac{b_1+b_2}{m_2}z_4\right),\end{aligned} \tag{24}$$

where $c_3 > 0$ is a constant control gain. It then follows that

$$\dot{e}_3 = -e_2 - c_3 e_3 - e_4.$$

Select the Lyapunov candidate $L_3 = L_2 + \frac{1}{2}e_3^2$. Its time derivative can be calculated by

$$\dot{L}_3 = -c_1 e_1^2 - c_2 e_2^2 - c_3 e_3^2 + e_3 e_4,$$

where $e_3 e_4$ is to be backstepped in the next step.

Step 4: The time derivative of e_4 can be calculated by

$$\begin{aligned}\dot{e}_4 =& \frac{b_1}{m_1 m_2}\dot{\xi}_2 - \dot{\alpha}_3\\ =& \frac{b_1 b_2}{m_1 m_2}\left(\frac{k_2}{m_3}z_3 + \frac{b_2}{m_3}z_4 - \frac{k_2}{m_3}z_5 - \frac{b_2+b_3}{m_3}z_6\right)\\ &+ \frac{b_1 k_2}{m_1 m_2}z_6 - \dot{\alpha}_3 + \frac{b_1 b_2}{m_1 m_2 m_3}u,\end{aligned}$$

where u is the control to be designed.

The control can be designed by

$$\begin{aligned}u =& \frac{m_1 m_2 m_3}{b_1 b_2}\Bigg(-e_3 - c_4 e_4 + \dot{\alpha}_3 - \frac{b_1 k_2}{m_1 m_2}z_6\\ &- \frac{b_1 b_2}{m_1 m_2}\left(\frac{k_2}{m_3}z_3 + \frac{b_2}{m_3}z_4 - \frac{k_2}{m_3}z_5 - \frac{b_2+b_3}{m_3}z_6\right)\Bigg),\end{aligned} \tag{25}$$

where $c_4 > 0$ is the control parameter. Select Lyapunov candidate $L_4 = L_3 + \frac{1}{2}e_4^2$; it follows that

$$\dot{L}_3 = -c_1 e_1^2 - c_2 e_2^2 - c_3 e_3^2 - c_4 e_4^2, \tag{26}$$

which ends the backstepping design.

3.3. Time derivatives of virtual controls

As can be seen from Section 3.2, the proposed control is given by (25), where virtual controls are given by (20) and (23). It should be noted in (23) and (25) that, before applying the proposed backstepping-based nonlinear control, derivatives of virtual controls (namely $\dot{\alpha}_1$ and $\dot{\alpha}_2$) should be calculated.

The time derivative of virtual control α_1 can be calculated by

$$\dot{\alpha}_1 = -c_1 \dot{e}_1 + \ddot{z}_{1r} = -c_1(z_2 - \dot{z}_{1r}) + \ddot{z}_{1r}, \tag{27}$$

where

$$\dot{z}_{1r} = \frac{\mathrm{d}\left(\frac{y_r}{k(t)}\right)}{\mathrm{d}t} = \frac{\dot{y}_r k - y_r \dot{k}}{k^2}, \tag{28}$$

$$\ddot{z}_{1r} = \frac{(\ddot{y}_r k - y_r \ddot{k})k^2 - 2k\dot{k}(\dot{y}_r k - y_r \dot{k})}{k^4}, \tag{29}$$

$$\dot{k} = -\sum_{i=1}^{3} K_i \omega_i \sin\left(\frac{2i\pi}{L}Vt\right) - K_7 \omega_7 \sin\left(\frac{14\pi}{L}Vt\right), \tag{30}$$

$$\ddot{k} = -\sum_{i=1}^{3} K_i \omega_i^2 \cos\left(\frac{2i\pi}{L}Vt\right) - K_7 \omega_7^2 \cos\left(\frac{14\pi}{L}Vt\right), \tag{31}$$

$$\omega_i = \frac{2i\pi}{L}V, \quad i = 1, 2, 3, 7. \tag{32}$$

The time derivative of virtual control α_2 can be calculated by

$$\dot{\alpha}_2 = -\dot{e}_1 - c_2 \dot{e}_2 + \frac{k_1+k}{m_1}\dot{z}_1 + \frac{\dot{k}}{m_1}z_1 + \frac{b_1}{m_1}\dot{z}_2 + \ddot{\alpha}_1, \tag{33}$$

where $\dot{e}_1$ can be calculated by

$$\dot{e}_1 = (z_2 - \dot{z}_{1r}), \tag{34}$$

and $\dot{z}_{1r}$ is calculated by (28); $\dot{e}_2$ can be calculated by

$$\dot{e}_2 = -\frac{k_1+k}{m_1}z_1 - \frac{b_1}{m_1}z_2 + \frac{k_1}{m_1}z_3 + \frac{b_1}{m_1}z_4 - \dot{\alpha}_1, \tag{35}$$

where $\dot{\alpha}_1$ is calculated by (27)–(31); $\dot{z}_1$ and $\dot{z}_2$ can be obtained by

$$\dot{z}_1 = z_2, \tag{36}$$

$$\dot{z}_2 = \dot{e}_2 + \dot{\alpha}_1, \tag{37}$$

where $\dot{e}_2$ is calculated by (35), and $\dot{\alpha}_1$ is calculated by (27); $\ddot{\alpha}_1$ can be calculated by

$$\ddot{\alpha}_1 = -c_1 \ddot{e}_1 + z_{1r}^{(3)} = -c_1(\dot{z}_2 - \ddot{z}_{1r}) + z_{1r}^{(3)}, \tag{38}$$

where $\dot{z}_2$ and $\ddot{z}_{1r}$ can be obtained respectively by (31) and (37). Denote $\ddot{z}_{1r}$ in (29) by

$$\ddot{z}_{1r} = \frac{\theta - \phi}{\psi},$$

where

$$\theta = (\ddot{y}_r k - y_r \ddot{k})k^2,$$

$\phi = 2k\dot{k}(\dot{y}_r k - y_r \dot{k}),$
$\psi = k^4.$

It follows that

$$z_{1r}^{(3)} = \frac{(\dot{\theta} - \dot{\phi})\psi - (\theta - \phi)\dot{\psi}}{\psi^2},$$

where

$$\dot{\theta} = \left(y_r^{(3)} k + \ddot{y}_r \dot{k} - \dot{y}_r \ddot{k} - y_r k^{(3)}\right) k^2 + 2k\dot{k}\left(\ddot{y}_r k - y_r \ddot{k}\right), \tag{39}$$

$$\dot{\phi} = 2k\dot{k}\left(\ddot{y}_r k - y_r \ddot{k}\right) + \left(\dot{y}_r k - y_r \dot{k}\right)\left(2\dot{k}^2 + 2k\ddot{k}\right), \tag{40}$$

$$\dot{\psi} = 4k^3 \dot{k}. \tag{41}$$

$$\dddot{k} = \sum_{i=1}^{3} K_i \omega_i^3 \sin(\frac{2i\pi}{L} Vt) + K_7 \omega_7^3 \sin(\frac{14\pi}{L} Vt). \tag{42}$$

The time derivative of α_3 can be calculated by

$$\dot{\alpha}_3 = -\dot{e}_2 - c_3 \dot{e}_3 - \frac{k_1}{m_1}\dot{z}_4 - \frac{b_1}{m_1}\left(\frac{k_1}{m_2}\dot{z}_1 + \frac{b_1}{m_2}\dot{z}_2 - \frac{k_1 + k_2}{m_2}\dot{z}_3 - \frac{b_1 + b_2}{m_2}\dot{z}_4\right) + \ddot{\alpha}_2, \tag{43}$$

where $\dot{e}_2$ can be calculated by (35); $\dot{e}_3$ can be calculated by

$$\dot{e}_3 = \frac{b_1}{m_1}\left(\frac{k_1}{m_2} z_1 + \frac{b_1}{m_2} z_2 - \frac{k_1 + k_2}{m_2} z_3 - \frac{b_1 + b_2}{m_2} z_4\right) + \frac{k_1}{m_1} z_4 - \dot{\alpha}_2 + \frac{b_1}{m_1}\frac{1}{m_2}\xi_2; \tag{44}$$

$\dot{z}_i$ $(i = 1, 2, 3, 4)$ can be calculated by using the state equations in (5).

In (43), the second-order derivative of α_2 in (43) can be calculated by

$$\ddot{\alpha}_2 = -\ddot{e}_1 - c_2 \ddot{e}_2 + \frac{k_1 + k}{m_1}\ddot{z}_1 + \frac{\dot{k}}{m_1}\dot{z}_1 + \frac{\ddot{k}}{m_1} z_1 + \frac{b_1}{m_1}\ddot{z}_2 + \dddot{\alpha}_1, \tag{45}$$

where

$$\ddot{e}_1 = \dot{z}_2 - \ddot{z}_{1r}, \quad \dot{z}_2 = \dot{e}_2 + \dot{\alpha}_1, \tag{46}$$

$$\ddot{e}_2 = -\frac{k_1 + k}{m_1}\dot{z}_1 - \frac{\dot{k}}{m_1} z_1 - \frac{b_1}{m_1}\dot{z}_2 + \frac{k_1}{m_1}\dot{z}_3 + \frac{b_1}{m_1}\dot{z}_4 - \ddot{\alpha}_1, \tag{47}$$

$$\ddot{z}_1 = \dot{z}_2, \quad \ddot{z}_2 = \ddot{e}_2 + \ddot{\alpha}_1, \tag{48}$$

$$\dddot{\alpha}_1 = -c_1(\dddot{z}_2 - \dddot{z}_{1r}) + z_{1r}^{(4)}, \tag{49}$$

$$z_{1r}^{(4)} = \frac{\ddot{\theta} - \ddot{\phi}}{\psi} - \frac{2(\dot{\theta} - \dot{\phi})\dot{\psi} + (\theta - \phi)\ddot{\psi}}{\psi^2} + \frac{2(\theta - \phi)\dot{\psi}^2}{\psi^3}. \tag{50}$$

Remark 8. It is implied from (27)–(50) that the derivatives of virtual controls can be explicitly calculated from system states and the reference contacting force.

3.4. Analysis on closed-loop system

The control algorithm can be summarized as following.

Algorithm 1.

(1) Calculate the virtual control α_1 with (20) and (28).
(2) Calculate the virtual control α_2 with (23) and (27)–(31).
(3) Calculate the virtual control α_3 with (24) and (33), where $\dot{e}_1$, $\dot{e}_2$, $\dot{z}_1$ and $\dot{z}_2$ are calculated with (34)–(37), and $\ddot{\alpha}_1$ is calculated with (38)–(42).
(4) Calculate the control u with (25), where some relevant terms can be calculated by (43)–(50).

Stability of the closed-loop system with the proposed control algorithm can be given by the following proposition.

Proposition 1. *Consider the pantograph–catenary system given by (1)–(4). Its reference contacting force is constant or time-varying continuous periodic. If the control is designed by Algorithm 1, then tracking error of the closed-loop system are globally asymptotically stable, and (13) is satisfied globally.*

Proof. Consider Lyapunov candidate L_4. It satisfies

$$\beta_1 \|e\|^2 \le L_4 \le \beta_2 \|e\|^2,$$

where $e \triangleq [e_1, e_2, e_3, e_4]^T$, $\beta_1 = \beta_2 = \frac{1}{2}$, and $\|\cdot\|$ denotes the Euclidean norm of vector or co-vector. The time derivative of L_4 along the closed-loop system with the control algorithm given in Algorithm 1 can be calculated by

$$\dot{L}_4 = -c_1 e_1^2 - c_2 e_2^2 - c_3 e_3^2 - c_4 e_4^2 \le -\beta_3 \|e\|^2, \tag{51}$$

where $\beta_3 = \min[c_1, c_2, c_3, c_4]$. Moreover,

$$\left\|\frac{\partial L_4}{\partial e}\right\| \le \beta_4 \|e\|,$$

where $\beta_4 = 1$. Consequently, according to Theorem 4.10 in [25], L_4 is a Lyapunov function, and e_1, e_2, e_3 and e_4 are globally asymptotically stable.

Based on (51), it can be obtained that

$$L_4(t) \le \mathrm{e}^{-\frac{\beta_3}{\beta_2} t} L_4(0),$$

and therefore,

$$\|e_1\| \le \|e\| \le \sqrt{\frac{1}{\beta_1} L_4(t)} \le \sqrt{\frac{1}{\beta_1}\mathrm{e}^{-\frac{\beta_3}{\beta_2} t} L_4(0)}, \tag{52}$$

indicating that (13) and (19) are satisfied.

Moreover, according to Proposition 4 in Appendix, z_3 and z_5 track periodic trajectories z_{3r} and z_{5r} asymptotically, and tracking errors $e_3^z \triangleq z_3 - z_{3r}$ and $e_5^z \triangleq z_5 - z_{5r}$ satisfy (70) in Appendix, where $\mathcal{L}_2(0) = 0$ and $\|\mathcal{L}_2(e)\| \le \kappa_3^z \|e\|$ with $\kappa_3^z > 0$.

Select a Lyapunov candidate $L_0 = L_4 + \frac{1}{2\gamma_3^z} {e_3^z}^2 + \frac{1}{2\gamma_5^z} {e_5^z}^2$ for the full-state closed-loop system, where $\gamma_3^z > 0$ and $\gamma_5^z > 0$. Its time derivative can be calculated by

$$\begin{aligned} \dot{L}_0 \le &- \beta_3 \|e\|^2 - \frac{k_1}{b_1 \gamma_3^z} {e_3^z}^2 + \frac{\kappa_3^z}{\gamma_3^z} e_3^z \|e\| - \frac{k_2}{b_2 \gamma_5^z} {e_5^z}^2 + \frac{\kappa_5^z}{\gamma_5^z} e_5^z \|e\| \\ = &- \left(\frac{1}{2}\beta_3 - \frac{{\kappa_3^z}^2 b_1}{4k_1 \gamma_3^z}\right)\|e\|^2 - \left(\sqrt{\frac{k_1}{b_1 \gamma_3^z}} e_3^z - \frac{\kappa_3^z}{2}\sqrt{b_1 k_1 \gamma_3^z}\|e\|\right)^2 \\ &- \left(\frac{1}{2}\beta_3 - \frac{{\kappa_5^z}^2 b_2}{4k_2 \gamma_5^z}\right)\|e\|^2 - \left(\sqrt{\frac{k_2}{b_2 \gamma_5^z}} e_5^z - \frac{\kappa_5^z}{2}\sqrt{b_2 k_2 \gamma_5^z}\|e\|\right)^2 \\ \le &0, \end{aligned}$$

where γ_3^z and γ_5^z can be selected appropriately such that

$$\left(\frac{1}{2}\beta_3 - \frac{{\kappa_3^z}^2 b_1}{4k_1 \gamma_3^z}\right) > 0, \quad \left(\frac{1}{2}\beta_3 - \frac{{\kappa_5^z}^2 b_2}{4k_2 \gamma_5^z}\right) > 0;$$

and $\dot{L}_0 = 0$ if and only if $e = 0$, $e_3^z = 0$ and $e_5^z = 0$.

Consequently, tracking errors of the closed-loop system with the proposed control are globally asymptotically stable. □

Remark 9. For more details about the principle and design process of backstepping, please see [25].

Remark 10. It should be noted that the system (1) (or (5)) is linear time-varying; consequently, the criteria of stability for time-varying system (e.g., Theorem 4.10 in [25]) should be used for closed-loop system analysis.

Remark 11. As can be seen from (52), performances of the closed-loop system can be tuned by control gains.

4. Partial-state feedback control

In practical applications, although its value can be obtained by using (3), the elasticity coefficient model (4) are usually unknown, indicating that $\dot{k}$, $\ddot{k}$, $\dddot{k}$ and $k^{(4)}$ cannot be directly calculated through the steps in Section 3. Moreover, velocities of the springs z_2, z_4 and z_6 are un-measurable; they cannot be used directly for state feedback.

In this section, it is supposed that the actual contacting force y, displacements z_1, z_3 and z_5 are measurable; differentiators and observers are designed to estimate the uncertain $\dot{k}$, $\ddot{k}$, $\dddot{k}$ and $k^{(4)}$, and un-measurable z_2, z_4 and z_6.

4.1. High-order differentiators for estimating $\dot{k}$, $\ddot{k}$ and $k^{(3)}$

It follows from (6) that $k(t)$ can be obtained by

$$k = \frac{y}{x_1}, \tag{53}$$

where $y = F_c$ and x_1 can be directly measured.

A simple high-order differentiator can be introduced to estimate time-derivatives of the elasticity coefficient:

$$\begin{cases} \dot{\zeta}_1 = \zeta_2, \\ \dot{\zeta}_2 = \zeta_3, \\ \dot{\zeta}_3 = \zeta_4, \\ \dot{\zeta}_4 = \zeta_5, \\ \dot{\zeta}_5 = R^5\left(-a_1(\zeta_1 - k(t)) - \frac{a_2}{R}\zeta_2 - \frac{a_3}{R^2}\zeta_3 - \frac{a_4}{R^3}\zeta_4 - \frac{a_5}{R^4}\zeta_5\right), \end{cases} \tag{54}$$

where a_i $(i = 1, 2, 3, 4, 5)$ and R are positive differentiator parameters to be tuned. For some recent detailed researches in differentiators, please refer to [26,27].

The time-derivatives of k are estimated by

$$\hat{k} = \zeta_1, \tag{55}$$

$$\hat{\dot{k}} = \zeta_2, \tag{56}$$

$$\hat{\ddot{k}} = \zeta_3, \tag{57}$$

$$\widehat{k^{(3)}} = \zeta_4, \tag{58}$$

$$\widehat{k^{(4)}} = \zeta_5. \tag{59}$$

Proposition 2. *With the differentiator (54), the time derivatives of the elasticity coefficient can be estimated by (56)–(59) with bounded estimation errors.*

Proof. It is obvious that (54) is an asymptotically stable linear system with a periodic input $k(t)$. Consequently, it can be claimed that ζ_1 tracks $k(t)$ with bounded tracking errors, which can be tuned arbitrarily small by assigning appropriate a_i $(i = 1, 2, 3, 4, 5)$ and R. It can be seen that ζ_i $(i = 2, 3, 4, 5)$ are time derivatives of ζ_1, and they are uniformly differentiable; as a result, they are capable of tracking time derivatives of k with bounded errors. □

Remark 12. Let $\tilde{\zeta}_i \triangleq \zeta_i - k^{(i-1)}$ $(i = 1, 2, 3, 4, 5)$, and $\tilde{\zeta} \triangleq [\tilde{\zeta}_1, \tilde{\zeta}_2, \tilde{\zeta}_3, \tilde{\zeta}_4, \tilde{\zeta}_5]^T$. It is apparent that estimation errors of the differentiator are input-to-state stable (ISS [25]) with respect to $k^{(i-1)}$ $(i = 2, 3, 4, 5)$. Moreover, there exists a positive function $L_5(\tilde{\zeta}_i)$ satisfying

$$\delta_1^d\|\tilde{\zeta}\|^2 \le L_5 \le \delta_2^d\|\tilde{\zeta}\|^2,$$
$$\dot{L}_5 \le -\delta_3^d\|\tilde{\zeta}\|^2 + \beta_d(\dot{k}, \ddot{k}, k^{(3)}, k^{(4)}),$$

where $\delta_i^d > 0$, $(i = 1, 2, 3)$, and β_d is a positive scalar satisfying $\beta_d(0, 0, 0, 0) = 0$.

Remark 13. It should be noted that $\hat{\dot{k}}$, $\hat{\ddot{k}}$, $\widehat{k^{(3)}}$, and $\widehat{k^{(4)}}$ are estimated values of $\dot{k}$, $\ddot{k}$, $k^{(3)}$, and $k^{(4)}$; they are different from derivatives $\dot{\hat{k}}$, $\ddot{\hat{k}}$, $\hat{k}^{(3)}$, and $\hat{k}^{(4)}$.

Remark 14. In this section, the high-order differentiator is applied to estimate derivatives of k. More detailed analysis on high-order differentiators can be found in [26] and [27].

4.2. Observer for z_2, z_4 and z_6

The observer for z_2, z_4 and z_6 can be designed by

$$\begin{cases} \dot{\hat{z}}_1 = \hat{z}_2 + l_1(\tilde{z}_1, \tilde{z}_3, \tilde{z}_5), \\ \dot{\hat{z}}_2 = -\frac{k_1+k(t)}{m_1}\hat{z}_1 - \frac{b_1}{m_1}\hat{z}_2 + \frac{k_1}{m_1}\hat{z}_3 + \frac{b_1}{m_1}\hat{z}_4 + l_2(\tilde{z}_1, \tilde{z}_3, \tilde{z}_5), \\ \dot{\hat{z}}_3 = \hat{z}_4 + l_3(\tilde{z}_1, \tilde{z}_3, \tilde{z}_5), \\ \dot{\hat{z}}_4 = \frac{k_1}{m_2}\hat{z}_1 + \frac{b_1}{m_2}\hat{z}_2 - \frac{k_1+k_2}{m_2}\hat{z}_3 - \frac{b_1+b_2}{m_2}\hat{z}_4 + \frac{k_2}{m_2}\hat{z}_5 \\ \quad + \frac{b_2}{m_2}\hat{z}_6 + l_4(\tilde{z}_1, \tilde{z}_3, \tilde{z}_5) \\ \dot{\hat{z}}_5 = \hat{z}_6 + l_5(\tilde{z}_1, \tilde{z}_3, \tilde{z}_5), \\ \dot{\hat{z}}_6 = \frac{k_2}{m_3}\hat{z}_3 + \frac{b_2}{m_3}\hat{z}_4 - \frac{k_2}{m_3}\hat{z}_5 - \frac{b_2+b_3}{m_3}\hat{z}_6 + l_6(\tilde{z}_1, \tilde{z}_3, \tilde{z}_5) + \frac{1}{m_3}u, \end{cases} \tag{60}$$

where z_1, z_3 and z_5 are outputs; $\hat{z}_i$ $(i = 1, 2, 3, 4, 5, 6)$ are estimations of z_i $(i = 1, 2, 3, 4, 5, 6)$; $\tilde{z}_i \triangleq \hat{z}_i - z_i$ $(i = 1, 2, 3, 4, 5, 6)$ are estimation errors; and

$$l_1(\tilde{z}_1, \tilde{z}_3, \tilde{z}_5) = -\varpi_1\tilde{z}_1,$$
$$l_2(\tilde{z}_1, \tilde{z}_3, \tilde{z}_5) = \left(\frac{k_1 + k(t)}{m_1} - \varpi_2\right)\tilde{z}_1 - \frac{k_1}{m_1}\tilde{z}_3,$$
$$l_3(\tilde{z}_1, \tilde{z}_3, \tilde{z}_5) = -\varpi_3\tilde{z}_3,$$
$$l_4(\tilde{z}_1, \tilde{z}_3, \tilde{z}_5) = -\frac{k_1}{m_2}\tilde{z}_1 + \left(\frac{k_1 + k_2}{m_2} - \varpi_4\right)\tilde{z}_3 - \frac{k_2}{m_2}\tilde{z}_5,$$
$$l_5(\tilde{z}_1, \tilde{z}_3, \tilde{z}_5) = -\varpi_5\tilde{z}_5,$$
$$l_6(\tilde{z}_1, \tilde{z}_3, \tilde{z}_5) = -\frac{k_2}{m_3}\tilde{z}_3 + \left(\frac{k_2}{m_3} - \varpi_6\right)\tilde{z}_5,$$

where $\varpi_i > 0$ $(i = 1, 2, 3, 4, 5, 6)$.

Proposition 3. *With the observer designed by (60), observation errors $\tilde{z}_i$ $(i = 1, 2, 3, 4, 5, 6)$ are globally exponentially stable.*

Proof. Subtracting (60) by (5) yields

$$\begin{cases} \dot{\tilde{z}}_1 = -\varpi_1\tilde{z}_1 + \tilde{z}_2, \\ \dot{\tilde{z}}_2 = -\varpi_2\tilde{z}_1 - \frac{b_1}{m_1}\tilde{z}_2 + \frac{b_1}{m_1}\tilde{z}_4, \\ \dot{\tilde{z}}_3 = -\varpi_3\tilde{z}_3 + \tilde{z}_4, \\ \dot{\tilde{z}}_4 = \frac{b_1}{m_2}\tilde{z}_2 - \varpi_4\tilde{z}_3 - \frac{b_1+b_2}{m_2}\tilde{z}_4 + \frac{b_2}{m_2}\tilde{z}_6, \\ \dot{\tilde{z}}_5 = -\varpi_5\tilde{z}_5 + \tilde{z}_6, \\ \dot{\tilde{z}}_6 = \frac{b_2}{m_3}\tilde{z}_4 - \varpi_6\tilde{z}_5 - \frac{b_1+b_2}{m_3}\tilde{z}_6. \end{cases} \tag{61}$$

Select a Lyapunov candidate

$$L_6^o = \frac{\varpi_2 m_1}{2}\tilde{z}_1^2 + \frac{m_1}{2}\tilde{z}_2^2 + \frac{\varpi_4 m_2}{2}\tilde{z}_3^2 + \frac{m_2}{2}\tilde{z}_4^2 + \frac{\varpi_6 m_3}{2}\tilde{z}_5^2 + \frac{m_3}{2}\tilde{z}_6^2.$$

Its time derivative can be calculated by

$$\begin{aligned}\dot{L}_6^o &= -\varpi_1\varpi_2 m_1\tilde{z}_1^2 - b_1\tilde{z}_2^2 + b_1\tilde{z}_2\tilde{z}_4 - \varpi_3\varpi_4 m_2\tilde{z}_3^2 - (b_1+b_2)\tilde{z}_4^2 \\ &\quad + b_1\tilde{z}_2\tilde{z}_4 + b_2\tilde{z}_4\tilde{z}_6 \\ &\quad - \varpi_5\varpi_6 m_3\tilde{z}_5^2 + b_2\tilde{z}_4\tilde{z}_6 - (b_2+b_3)\tilde{z}_6^2 \\ &= -\varpi_1\varpi_2 m_1\tilde{z}_1^2 - b_1\left(\tilde{z}_2 - \tilde{z}_4\right)^2 - \varpi_3\varpi_4 m_2\tilde{z}_3^2 \\ &\quad - b_2(\tilde{z}_4 - \tilde{z}_6)^2 - b_3\tilde{z}_6^2 - \varpi_5\varpi_6 m_3\tilde{z}_5^2 \\ &\le 0\end{aligned}$$

where $\dot{L}_6^o = 0$ if and only if $\tilde{z} \triangleq [\tilde{z}_1, \tilde{z}_2, \tilde{z}_3, \tilde{z}_4, \tilde{z}_5, \tilde{z}_6]^T = 0$.

Consequently, the observation errors are globally asymptotically stable. It is apparent that (61) is a time-invariant linear system; therefore, the observation errors are globally exponentially stable. □

With the proposed observer (60), the un-measurable z_2, z_4 and z_6 can be re-constructed by $\hat{z}_2$, $\hat{z}_4$ and $\hat{z}_6$.

Remark 15. According to Lyapunov converse theorem [25], there exists a Lyapunov function L_6 for the exponentially stable linear system (61), such that

$$\delta_1^{ob}\|\tilde{z}\|^2 \le L_6^o(\tilde{z}) \le \delta_2^{ob}\|\tilde{z}\|^2,$$

$$\dot{L}_6^o(\tilde{z}) \le -\delta_3^{ob}\|\tilde{z}\|^2,$$

where $\delta_i^{ob} > 0,\ (i = 1, 2, 3)$.

Remark 16. More detailed information of tracking by using observers can be found in [28].

4.3. Stability of the closed-loop system with observers

With the observer (54) and (60), the un-measurable $\dot{k}$, $\ddot{k}$, $\dddot{k}$, $k^{(4)}$, z_2, z_4 and z_6 can be reconstructed, and the control algorithm can be summarized as following.

Algorithm 2.

(1) Calculate the virtual control α_1 with (20) and (28), where $\dot{k}$ should be replaced by $\hat{\dot{k}}$ in (56), and k is calculated by (53).
(2) Calculate the virtual control α_2 with (23) and (27)–(29), where $\dot{k}$ and $\ddot{k}$ should be replaced by $\hat{\dot{k}}$ in (56) and $\hat{\ddot{k}}$ in (57), respectively; and k is calculated by (53). z_2 is reconstructed by $\hat{z}_2$ in (60).
(3) Calculate the control α_3 with (25) and (33), where $\dot{e}_1$, $\dot{e}_2$, $\dot{z}_1$ and $\dot{z}_2$ are calculated with (34)–(37); $\ddot{\alpha}_1$ is calculated by (38)–(41); k is calculated by (53); $\dot{k}$, $\ddot{k}$ and $k^{(3)}$ are replaced by $\hat{\dot{k}}$ in (56), $\hat{\ddot{k}}$ in (57) and $\widehat{k^{(3)}}$ in (58), respectively; and z_2 and z_4 are reconstructed by $\hat{z}_2$ and $\hat{z}_4$ in (60).
(4) Calculate the control u with (25), where derivatives of virtual controls can be calculated by (43)–(50); k is calculated by (53); $\dot{k}$, $\ddot{k}$, $k^{(3)}$, $k^{(4)}$ are replaced by $\hat{\dot{k}}$, $\hat{\ddot{k}}$, $\widehat{k^{(3)}}$, $\widehat{k^{(4)}}$ in (56)–(59), respectively; and z_2, z_4 and z_6 are reconstructed by $\hat{z}_2$, $\hat{z}_4$ and $\hat{z}_6$ in (60).

Stability of the closed-loop system with uncertain parameters and unmeasurable states can be given by the following theorem.

Theorem 1. *Consider the pantograph–catenary system given by (1)–(4), where the elasticity coefficient model is unknown, and displacement variations $\dot{x}_1$, $\dot{x}_2$, and $\dot{x}_3$ are unmeasurable. Suppose that the reference contacting force is constant or continuously periodic. The control is designed by Algorithm 2, with time derivatives of $k(t)$ estimated by the differentiator (54), and with the unmeasurable z_2, z_4, and z_6 reconstructed by the observer (60). Then, tracking errors of the closed-loop system are ultimately bounded with tunable ultimate bounds, and (13) is satisfied.*

Proof. Consider that $\dot{k}$, $\ddot{k}$, $k^{(3)}$, $k^{(4)}$, z_2, z_4, and z_6 are reconstructed by (54) and (60), respectively. It follows that the tracking error dynamics can be given by

$$\begin{cases}\dot{e}_1 = -c_1 e_1 + e_2 + o_1(\tilde{z}, \tilde{\zeta}), \\ \dot{e}_2 = -e_1 - c_2 e_2 + e_3 + o_2(\tilde{z}, \tilde{\zeta}), \\ \dot{e}_3 = -e_2 - c_3 e_3 + e_4 + o_3(\tilde{z}, \tilde{\zeta}), \\ \dot{e}_4 = -e_3 - c_4 e_4 + o_4(\tilde{z}, \tilde{\zeta}),\end{cases} \tag{62}$$

where $\tilde{\zeta} \triangleq [\tilde{\zeta}_1, \tilde{\zeta}_2, \tilde{\zeta}_3, \tilde{\zeta}_4, \tilde{\zeta}_5]^T$; $o_1(\tilde{z})$, $o_2(\tilde{z})$, $o_3(\tilde{z})$ and $o_4(\tilde{z})$ are errors resulted from differentiator errors and observation errors, and they satisfy

$$o_1(0,0) = 0,\ o_2(0,0) = 0,\ o_2(0,0) = 0,\ o_2(0,0) = 0.$$

Since $\dot{k}$, $\ddot{k}$, $k^{(3)}$, $k^{(4)}$ are continuously bounded, and $\tilde{\zeta}$ and $\tilde{z}$ are bounded, there exist positive κ_{ij} $(i = 1, 2, 3, 4,\ j = 1, 2)$ such that the following expressions hold locally:

$$\begin{aligned}&\|o_1(\tilde{z}, \tilde{\xi})\| \le \kappa_{11}\|\tilde{z}\| + \kappa_{12}\|\tilde{\zeta}\|, \\ &\|o_2(\tilde{z}, \tilde{\xi})\| \le \kappa_{21}\|\tilde{z}\| + \kappa_{22}\|\tilde{\zeta}\|, \\ &\|o_3(\tilde{z}, \tilde{\xi})\| \le \kappa_{31}\|\tilde{z}\| + \kappa_{32}\|\tilde{\zeta}\|, \\ &\|o_4(\tilde{z}, \tilde{\xi})\| \le \kappa_{41}\|\tilde{z}\| + \kappa_{42}\|\tilde{\zeta}\|.\end{aligned} \tag{63}$$

It follows that the time derivative of L_4 can be calculated by

$$\begin{aligned}\dot{L}_4 &= -c_1 e_1^2 - c_2 e_2^2 - c_3 e_3^2 - c_4 e_4^2 + e_1 o_1 + e_2 o_2 + e_3 o_3 + e_4 o_4 \\ &\le -\sum_{i=1}^{4}\left(c_i e_i^2 + \kappa_{i1}\|e_i\tilde{z}\| + \kappa_{i2}\|e_i\tilde{\zeta}\|\right).\end{aligned}$$

Select the Lyapunov candidate $L_7 = L_4 + \gamma_d L_5 + \gamma_{ob} L_6$ with $\gamma_d > 0$ and $\gamma_{ob} > 0$. Its time derivative can be calculated by

$$\begin{aligned}\dot{L}_7 &\le \sum_{i=1}^{4}\left(-c_i e_i^2 + \kappa_{i1}\|e_i\tilde{z}\| + \kappa_{i2}\|e_i\tilde{\zeta}\|\right) \\ &\quad - \gamma_{ob}\delta_3^{ob}\|\tilde{z}\|^2 - \gamma_d\delta_3^d\|\tilde{\zeta}\|^2 + \gamma_d\beta_d \\ &= -\sum_{i=1}^{4}(c_i - 2\eta_i)\,e_i^2 + \gamma_d\beta_d - \sum_{i=1}^{4}\left(\gamma_{ob}\delta_3^{ob} - \frac{\kappa_{i1}^2}{4\eta_i}\right)\tilde{z}_i^2 \\ &\quad - \sum_{i=1}^{4}\left(\sqrt{\eta_i}e_i - \frac{\kappa_{i1}}{2\sqrt{\eta_i}}\tilde{z}\right)^2 \\ &\quad - \sum_{i=1}^{4}\left(\gamma_d\delta_3^d - \frac{\kappa_{i2}^2}{4\eta_i}\right)\tilde{\zeta}_i^2 - \sum_{i=1}^{4}\left(\sqrt{\eta_i}e_i - \frac{\kappa_{i2}}{2\sqrt{\eta_i}}\tilde{\zeta}\right)^2 \\ &\le -\sum_{i=1}^{4}(c_i - 2\eta_i)\,e_i^2 + \gamma_d\beta_d - \sum_{i=1}^{4}\left(\gamma_{ob}\delta_3^{ob} - \frac{\kappa_{i1}^2}{4\eta_i}\right)\tilde{z}_i^2 \\ &\quad - \sum_{i=1}^{4}\left(\gamma_d\delta_3^d - \frac{\kappa_{i2}^2}{4\eta_i}\right)\tilde{\zeta}_i^2\end{aligned}$$

where $0 < 2\eta_i < c_1$ $(i = 1, 2, 3)$; $\gamma_{ob} > 0$ and $\gamma_d > 0$ can be selected large enough, such that $\gamma_{ob}\delta_3^{ob} - \frac{\kappa_{i1}^2}{4\eta_i} > 0$ and $\gamma_d\delta_3^d - \frac{\kappa_{i2}^2}{4\eta_i} > 0$.

Then, it can be claimed that L_7 satisfies

$$\delta_1\|\bar{e}\|^2 \le L_7 \le \delta_2\|\bar{e}\|^2, \tag{64}$$

$$\dot{L}_7 \le -\delta_3\|\bar{e}\| + \gamma_d\beta_d(\dot{k}, \ddot{k}, k^{(3)}, k^{(4)}), \tag{65}$$

where $\bar{e} \triangleq [e^T, \tilde{z}^T, \tilde{\zeta}^T]^T$, and

$$\delta_1 = \min\left[\frac{1}{2}, \gamma_{ob}\delta_1^{ob}, \gamma_d\delta_1^d\right], \quad \delta_2 = \max\left[\frac{1}{2}, \gamma_{ob}\delta_2^{ob}, \gamma_d\delta_2^d\right],$$

$$\delta_3 = \min_{i=1,2,3,4}\left[c_i - 2\eta_i,\ \gamma_{ob}\delta_3^{ob} - \frac{\kappa_{i1}^2}{4\eta_i},\ \gamma_d\delta_3^d - \frac{\kappa_{i2}^2}{4\eta_i}\right].$$

Consequently, it can be concluded that $\bar{e}$ is ISS with respect to $k^{(i)}$ $(i = 1, 2, 3, 4)$.

Since $k(t)$ is periodic, it follows that $k^{(i)}$ $(i = 1, 2, 3, 4)$ are periodic and bounded, and it holds that

$$\beta_d(\dot{k}, \ddot{k}, k^{(3)}, k^{(4)}) \le \bar{\beta}_d, \tag{66}$$

where $\bar{\beta}_d > 0$ denotes the bound of β_d. It can be solved from (64) and (65) that

$$L_7(t) \le e^{-\frac{\delta_3}{\delta_2}t}\left(L_7(0) - \frac{\delta_2\gamma_d\bar{\beta}_d}{\delta_3}\right) + \frac{\delta_2\gamma_d\bar{\beta}_d}{\delta_3},$$

and therefore,

$$\|e_1\| \le \sqrt{\frac{1}{\delta_1}e^{-\frac{\delta_3}{\delta_2}t}\left(L_7(0) - \frac{\delta_2\gamma_d\bar{\beta}_d}{\delta_3}\right) + \frac{\delta_2\gamma_d\bar{\beta}_d}{\delta_1\delta_3}}, \tag{67}$$

which can be tuned by assigning appropriate δ_i $(i = 1, 2, 3)$.

Moreover, according to Proposition 5 in Appendix, z_3 (and z_5) tracks a periodic trajectory z_{3r} (and z_{5r}) asymptotically, and its tracking error $e_3^z \triangleq z_3 - z_{3r}$ ($e_5^z \triangleq z_5 - z_{5r}$) satisfies (71) in Appendix, where $\mathcal{L}_3(0) = 0$ and $\|\mathcal{L}_3(\bar{e})\| \le \beta_3^z\|\bar{e}\|$ with $\beta_3^z > 0$.

Select a Lyapunov candidate $L_0^{ob} = L_7 + \frac{1}{2\gamma_3^z}{e_3^z}^2 + \frac{1}{2\gamma_5^z}{e_5^z}^2$ for the full-state closed-loop system with observers, where $\gamma_3^z > 0$ and $\gamma_5^z > 0$. Its time derivative can be calculated by

$$\begin{aligned}
\dot{L}_0^{ob} &\le -\delta_3\|\bar{e}\|^2 - \frac{k_1}{b_1\gamma_3^z}{e_3^z}^2 + \frac{\beta_3^z}{\gamma_3^z}e_3^z\|\bar{e}\| \\
&\quad - \frac{k_2}{b_2\gamma_5^z}{e_5^z}^2 + \frac{\beta_5^z}{\gamma_5^z}e_5^z\|\bar{e}\| + \gamma_d\bar{\beta}_d \\
&= -\left(\delta_3 - \frac{{\beta_3^z}^2 b_1}{4k_1\gamma_3^z} - \frac{{\beta_5^z}^2 b_2}{4k_2\gamma_5^z}\right)\|\bar{e}\|^2 + \gamma_d\bar{\beta}_d \\
&\quad - \left(\sqrt{\frac{k_1}{b_1\gamma_3^z}}e_3^z - \frac{\beta_3^z}{2}\sqrt{b_1 k_1\gamma_3^z}\|\bar{e}\|\right)^2 \\
&\quad - \left(\sqrt{\frac{k_2}{b_2\gamma_5^z}}e_5^z - \frac{\beta_5^z}{2}\sqrt{b_2 k_2\gamma_5^z}\|\bar{e}\|\right)^2
\end{aligned}$$

where γ_3^z and γ_5^z can be selected large enough such that $\left(\delta_3 - \frac{{\beta_3^z}^2 b_1}{4k_1\gamma_3^z} - \frac{{\beta_5^z}^2 b_2}{4k_2\gamma_5^z}\right) > 0$. As a consequence, tracking errors of the closed-loop system with the proposed control and observers are ultimately bounded with tunable ultimate bounds. □

5. Simulations and discussion

In the simulations, values of parameters of the pantograph–catenary system are taken from [6,9,11], as listed in Table 1. The train speed is set to $V = 90$ m/s to test performances of the closed-loop system with high speed. The reference contact force is set by 100N. Initial values of system states are given by

$$[x_1(0), \dot{x}_1(0), x_2(0), \dot{x}_2(0), x_3(0), \dot{x}_3(0)]^T$$

$$= [0.005, 0, 0.01, 0, 0.01, 0]^T.$$

Table 1
Values of parameters.

Notations	Values	Notations	Values
k_1	7015.9 Nm^{-1}	L	65 m
m_1	8 kg	m_2	12 kg
b_1	120 Nsm^{-1}	b_2	30 Nsm^{-1}
V	90 ms^{-1}	K_0	7000 Nm^{-1}
K_1	3360 Nm^{-1}	K_2	650 Nm^{-1}
K_3	160 Nm^{-1}	K_7	160 Nm^{-1}
k_2	1550.1 Nm^{-1}		

Table 2
Values of control gains and observer gains.

Notations	Values	Notations	Values
c_1	12	a_1	128
c_2	36	a_2	128
c_3	108	a_3	64
c_4	324	a_4	32
R	200	a_5	4
ϖ_1	20	ϖ_2	4
ϖ_3	20	ϖ_4	4
ϖ_5	20	ϖ_6	4

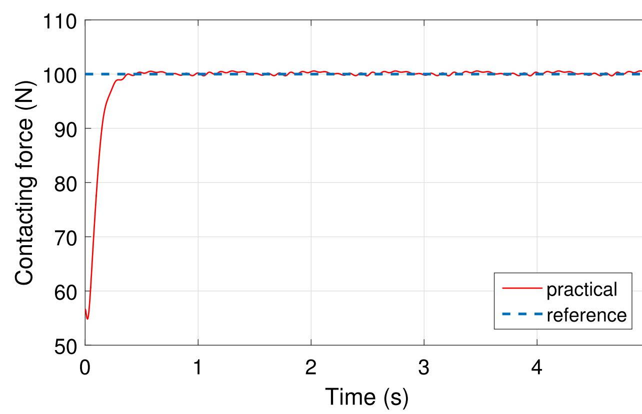

Fig. 3. Contact force with full-state feedback control: the tracking error is globally exponentially stable.

Suppose that elasticity coefficient model is fully known in priori, and z_2, z_4 and z_6 are measurable. In this case, Algorithm 1 is applied, with control gains listed in Table 2. The tracking performance of the closed-loop system with respect to a constant contacting force is illustrated by Fig. 3. As can be seen, the tracking error is globally asymptotically stable, and the transient process is satisfactory.

In more practical applications, the accurate model of elasticity coefficient $k(t)$ is unknown, and z_2, z_4 and z_6 are unmeasurable, implying that the elasticity coefficient model (4), as well as the unmeasurable z_2, z_4, and z_6, cannot be used directly in control design. In this case, Algorithm 2 is applied with control gains, differentiator parameters and observer gains listed in Table 2. Initial values of observer states are all set to zeros. It can be seen from Fig. 4 that, with the proposed partial-state feedback control algorithm, the closed-loop system is capable of tracking the reference contacting force with ultimately bounded tracking errors. The displayed bounded tracking is in significant accordance with the theoretical results. It can be seen from Figs. 5–7 that reconstructed signals $\hat{z}_2$, $\hat{z}_4$, $\hat{z}_6$ are capable of tracking their actual values exponentially. The control signal is displayed in Fig. 8, where it can be seen that the controller is fairly implementable.

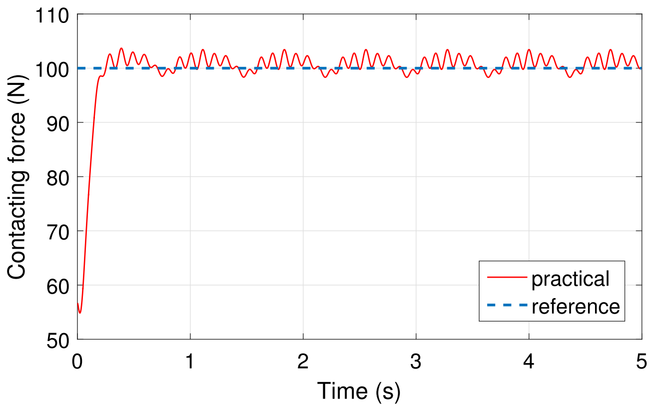

Fig. 4. Contact force with the proposed partial-state feedback control: the tracking error is ultimately bounded.

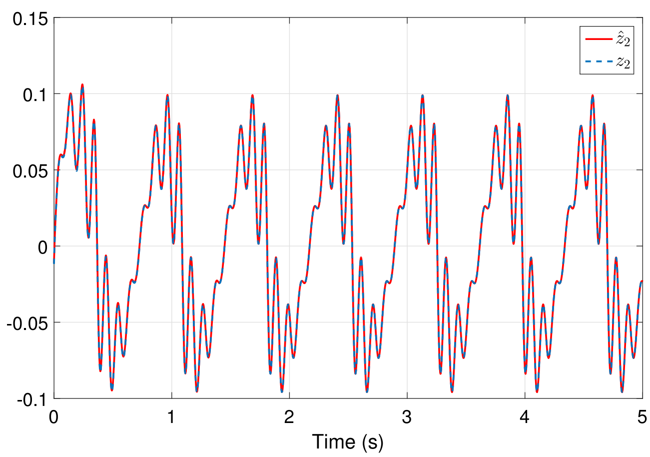

Fig. 5. Observed z_2: the observation error is globally exponentially stable.

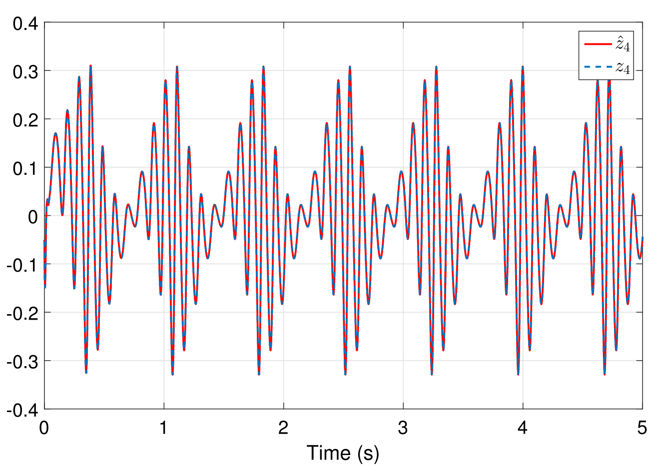

Fig. 6. Observed z_4: the observation error is globally exponentially stable.

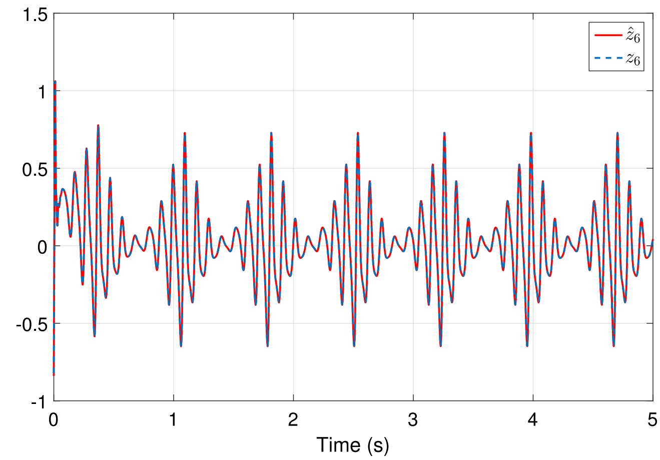

Fig. 7. Observed z_6: the observation error is globally exponentially stable.

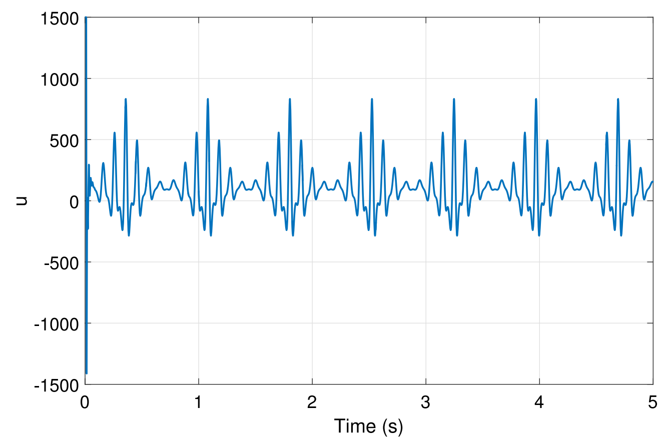

Fig. 8. Control signal of the closed-loop system with the proposed partial-state feedback.

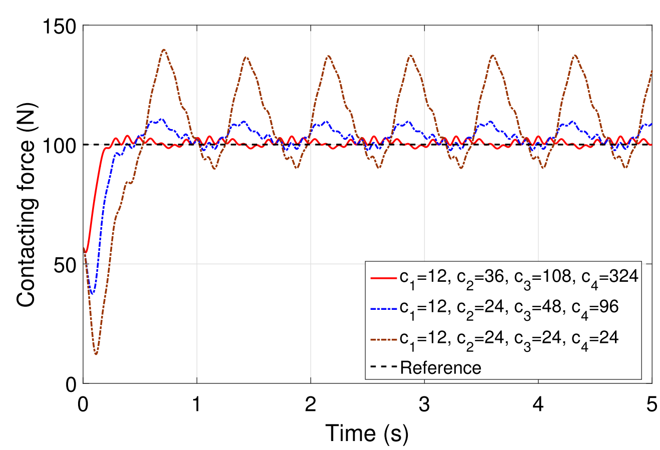

Fig. 9. Comparison of closed-loop performances with different control gains.

The ultimate bound in (67) cannot be calculated explicitly, since it is related to the differentiator error β_d in (65). The train is supposed to be operated in very high speed (90 m/s in this simulation), such that the frequency of periodic catenary stiffness $k(t)$ is very high, and the tracking error of the differentiator would be considerably large. The existence of β_d is obvious; however, its value is difficult to be determined explicitly. Even though we cannot calculate the particular value of ultimate bound explicitly, it can be tuned by control parameters. According to (67), δ_1, δ_2 and δ_3 are related directly to control gains c_1, c_2, c_3 and c_4. To illustrate, a comparison of closed-loop performance with different control gains is given in Fig. 9, where it can be seen that large control gains would lead to smaller ultimate bounds.

Remark 17. In simulation, the closed-loop system is not ideally continuous. Both the model and the controller are discretized with small sampling intervals. Consequently, the control gains cannot be increased to extremely large values to reduce the chattering. If the control gains are extremely large and the trains speed is high, there would be stability problems due to the discretization.

6. Conclusion

In this paper, a nonlinear partial-state feedback control is proposed for a 3-DOF pantograph–catenary system, such that the contact force between pantograph and catenary can track a continuous reference force. The proposed control is designed based on backstepping approach, where time derivatives of virtual controls are calculated explicitly. A high-order differentiator is designed for estimating derivatives of time-varying elasticity coefficient, and an observer is designed to reconstruct the unmeasurable spring velocities. Ultimate boundedness of tracking errors of the closed-loop system with proposed control and observer is proved rigorously. Theoretical results are demonstrated by numerical simulation.

It should be noted that the approach proposed in this paper is open for further extensions (for example, adaptive control in case of parametric uncertainties. For more details, please see the canonical design process in [24]).

Acknowledgments

This research is supported by National Natural Science Foundation of China under Grant No. 61703018, and the Young Elite Scientists Sponsorship Program by CAST, China under Grant 2017QNR C001.

Conflict of interest

There is no conflict of interest.

Appendix. Tracking performance of z_3 in Proposition 1 and Theorem 1

Proposition 4. *Suppose that the reference contacting force is constant or continuously periodic. Then, in the closed-loop system with Algorithm 1, z_3 (and z_5) tracks a periodic trajectory asymptotically.*

Proof. It follows from definition of e_3 that

$$\begin{aligned}\xi_1 &= e_3 + \alpha_2\\ &= e_3 - e_1 - c_2 e_2 + \frac{k_1+k}{m_1}(e_1 + z_{1r}) + \frac{b_1}{m_1}(e_2+\alpha_1) + \dot{\alpha}_1\\ &= \mathcal{L}_1(e) + \frac{k_1}{m_1} z_{1r} + \frac{1}{m_1} y_r + \frac{b_1}{m_1}\alpha_1 + \dot{\alpha}_1\\ &= \mathcal{L}_1(e) + \mathcal{P}_1 + \frac{b_1}{m_1}(-c_1 e_1 + \dot{z}_{1r}) - c_1\dot{e}_1 + \ddot{z}_{1r}\\ &= \mathcal{L}_2(e) + \mathcal{P}_2,\end{aligned} \tag{68}$$

where $\mathcal{L}_1(e)$ and $\mathcal{L}_2(e)$ are linear combinations of e_1, e_2 and e_3, and it holds that $\|\mathcal{L}_2(e)\| \le \kappa_3^z\|e\|$ with some certain $\kappa_3^z > 0$; $\mathcal{P}_1$ and $\mathcal{P}_2$ are continuously periodic terms.

Let z_{3r} be the solution of the following system:

$$\dot{z}_{3r} = -\frac{k_1}{b_1} z_{3r} + \frac{1}{b_1}\mathcal{P}_2, \tag{69}$$

which is a stable linear time-invariant system plus a periodic input. It is apparent that z_{3r} is ultimately periodic.

Let $e_3^z \triangleq z_3 - z_{3r}$. It follows from (17), (68) and (69) that

$$\dot{e}_3^z = -\frac{k_1}{b_1} e_3^z + \frac{1}{b_1}\mathcal{L}_2(e), \tag{70}$$

where e decreases exponentially according to (52). Consequently, it can be claimed that $e_3^z \to 0$, indicating that z_3 tracks a periodic trajectory asymptotically.

With similar steps, it can be proved that z_5 tracks a periodic trajectory asymptotically. □

Proposition 5. *Suppose that the reference contacting force is constant or continuously periodic. Then, in the closed-loop system with Algorithm 2, z_3 (and z_5) tracks a periodic trajectory asymptotically.*

Proof. The proof is similar to that of Proposition 4. It can be proved that ζ_1 can be expressed as the sum of $\mathcal{L}_3(\bar{e})$ and $\mathcal{P}_3$, where $\mathcal{L}_3(\bar{e})$ is a linear combination of e and $\tilde{z}$, and $\mathcal{P}_3$ is composed by continuously periodic terms. It holds that $\|\mathcal{L}_3(\bar{e})\| \le \beta_3^z\|\bar{e}\|$ with a certain $\beta_3^z > 0$. It follows that

$$\dot{e}_3^z = -\frac{k_1}{b_1} e_3^z + \mathcal{L}_3(\bar{e}), \tag{71}$$

and $e_3^z \to 0$ (since $\bar{e}$ vanishes), indicating that z_3 tracks a periodic trajectory asymptotically.

With similar steps, it can be proved that z_5 tracks a periodic trajectory asymptotically. □

References

[1] Jimenez-Octavio JR, Sanchez-Rebollo C, Carnicero A. The dependance on mechanical design in railway electrification. IEEE Electrif Mag 2013;1(1):4–10.
[2] Ambrosio J, Pombo J, Pereira M, Antunes P, Mosca A. A computational procedure for the dynamic analysis of the catenary-pantograph interaction in high-speed trains. J Theoret Appl Mech 2012;50(3):681–99.
[3] Chen Z, Wang T, Hui L, Guo F. Determination of the optimal contact load in pantograph–catenary system. Trans China Electrotech Soc 2013;28(6):86–92 [in Chinese].
[4] Sanchez-Rebollo C, Jimenez-Octavio JR, Carnicero A. Active control strategy on a cantenary-pantograph validated model. Veh Syst Dyn 2013;51(4):554–69.
[5] Lin Y, Lin C, Yang C. Robust active vibration control for rail vehicle pantograph. IEEE Trans Veh Technol 2007;56(4):1994–2004.
[6] Ide CK, Olaru S, Rodriguez-Ayerbe P, Rachid A. A nonlinear state feedback control approach for a Pantograph-Catenary system. In: Proceedings of the 17th international conference on system theory, control and computing. IEEE; 2013, p. 268–73.
[7] Pisano A, Usai E. Output-feedback regulation of the contact force in high-speed train pantographs. J Dyn Syst Meas Control 2004;126(1):82–7.
[8] Chater E, Ghani D, Giri F, Haloua M. Output feedback control of pantograph–catenary system with adaptive estimation of catenary parameters. J Modern Transp 2015;23(4):252–61.
[9] Taran M, Rodriguez-Ayerbe P, Olaru S, Ticlea A. Moving horizon control and estimation of a pantograph-Catenary system. In: Proceedings of the 17th international conference on system theory, control and computing. IEEE; 2013, p. 527–32.
[10] Balestrino A, Bruno O, Landi A, Sani L. Innovative solutions for overhead catenary-pantograph system: wire acturated control and observerd contact force. Veh Syst Dyn 2000;33(2):69–89.
[11] Pisano A, Usai E. Contact force estimation and regulation in active pantographs: an algebraic observability approach. Asian J Control 2011;13(6):761–72.
[12] Allotta B, Pugi L, Bartolini F. Design and experimental results of an active suspension system for a high-speed pantograph. IEEE/ASME Trans Mechatronics 2008;13(5):548–57.
[13] Rachid A. Pantograph catenary control and observation using the LMI approach. In: Proceedings of the 50th IEEE conference on decision and control and European control conference. IEEE; 2011, p. 2287–92.
[14] Chen M, Ward CP, Hubbard EM, Hubbard P. Modelling and active control design of trolleybus catenary-pantograph system. IFAC-PapersOnLine 2016;49–21:282–7.
[15] Song Y, Ouyang H, Liu Z, Mei G, Wang H, Lu X. Active control of contact force for high-speed railway pantograph–catenary based on multi-body pantograph model. Mech Mach Theory 2017;115:35–59.

[16] Mokrani N, Rachid A, Rami MA. A tracking control for pantograph–catenary system. In: Proceedings of 2015 IEEE 54th annual conference on decision and control (CDC). Osaka (Japan); 2015. p. 185–90.
[17] Allotta B, Papi M, Pugi L, Toni P, Violi AG. Experimental campaign on a servo-actuated pantograph. In: Proceedings of international conference on advanced intelligent mechatronics. IEEE/ASME; 2001, p. 237–42.
[18] Cho YH. Numerical simulation of the dynamic responses of railway overhead contact lines to a moving pantograph, considering a nonlinear dropper. J Sound Vib 2008;315:433–54.
[19] Bucca G, Collina A. A procedure for the wear prediction of collector strip and contact wire in pantograph–catenary system. Wear 2009;266:46–59.
[20] Lim SC, Ashby MF. Wear-mechanicsm maps. Acta Metall 1987;35(1):1–24.
[21] Holm R, Holm E. Electric contacts handbook. Berlin: Springer-verlag; 1958.
[22] Levant A, Pisano A, Usai E. Output-feedback control of the contact-force in high-speed-train pantograph. In: Proceedings of the 40th IEEE conference on decision and control. Orlando (USA); 2001. p. 1831–6.
[23] British Standards Institution. Railway applications - current collection systems - validation of simulation of the dynamic interaction between pantograph and overhead contact line. London, British Standards Institution; 2002, BS EN 50318:2002.
[24] Krstic M, Kanellakopoulos I, Kokotovic P. Nonlinear and adaptive control design. Inc.: John Wiley & Sons; 1995.
[25] Khalil H. Nonlinear systems. 3rd ed. New Jercey: Prentice Hall Inc.; 2002.
[26] Bu X, Wu X, Zhang R, Ma Z, Huang J. Tracking differentiator design for the robust backstepping control of a flexible air-breathing hypersonic vehicle. J Franklin Inst B 2015;352(4):1739–65.
[27] Wang X, Chen Z, Yuan Z. Design and analysis for new discrete tracking-differentiators. Appl Math 2003;18(2):214–22.
[28] Nunes EVL, Peixoto AJ, Oliveira TR, Hsu L. Global exact tracking for uncertain MIMO linear systems by output feedback sliding mode control. J Franklin Inst B 2014;351(4):2015–32.